BIOCHEMISTRY
including biophysical chemistry & molecular biology

Article

pubs.acs.org/biochemistry

Reconstitution of the Platelet Glycoprotein Ib-IX Complex in Phospholipid Bilayer Nanodiscs

Rong Yan,[†,‡] Xi Mo,[‡] Angel M. Paredes,[§] Kesheng Dai,[†] Francois Lanza,[∥] Miguel A. Cruz,[⊥] and Renhao Li*[,‡,@]

[†]Ministry of Health Key Laboratory of Thrombosis and Haemostasis, Jiangsu Institute of Hematology, First Affiliated Hospital of Soochow University, Suzhou, China

[‡]Center for Membrane Biology, Department of Biochemistry and Molecular Biology, and [§]Department of Pathology and Laboratory Medicine, The University of Texas Health Science Center at Houston, Houston, Texas 77030, United States

[∥]Etablissement de Transfusion Sanguine, INSERM, Unite311, Strasbourg Cedex, France

[⊥]Thrombosis Research Section, Department of Medicine, Baylor College of Medicine, Houston, Texas 77030, United States

[@]Department of Pediatrics, Division of Hematology/Oncology, Aflac Cancer Center and Blood Disorders Service, Emory University School of Medicine, Atlanta, Georgia 30322, United States

Supporting Information

ABSTRACT: The glycoprotein Ib-IX (GPIb-IX) complex expressed on platelet plasma membrane is involved in thrombosis and hemostasis via the initiation of adhesion of platelets to von Willebrand factor (VWF) exposed at the injured vessel wall. While most of the knowledge of the GPIb-IX complex was obtained from studies on platelets and transfected mammalian cells expressing the GPIb-IX complex, there is not an in vitro membrane system that allows systematic analysis of this receptor. The phospholipid bilayer Nanodisc composed of a patch of phospholipid surrounded by membrane scaffold protein is an attractive tool for membrane protein study. We show here that the GPIb-IX complex purified from human platelets has been reconstituted into the Nanodisc. The Nanodisc-reconstituted GPIb-IX complex was able to bind various conformation-sensitive monoclonal antibodies. Furthermore, it bound to VWF in the presence of botrocetin with an apparent K_d of 0.73 ± 0.07 nM. The binding to VWF was inhibited by anti-GPIbα antibodies with epitopes overlapping with the VWF-binding site, but not by anti-GPIbβ monoclonal antibody RAM.1. Finally, the Nanodisc-reconstituted GPIb-IX complex exhibited ligand binding activity similar to that of the isolated extracellular domain of GPIbα. In conclusion, the GPIb-IX complex in Nanodiscs adopts a native-like conformation and possesses the ability to bind its natural ligands, thus making a Nanodisc a suitable in vitro platform for further investigation of this hemostatically important receptor complex.

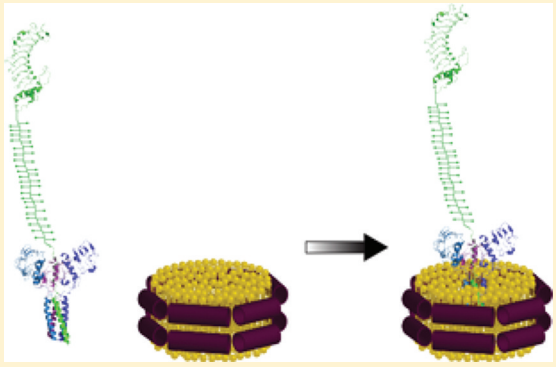

Cell adhesion receptors not only mediate cell−matrix interactions and cell−cell contacts through ligand binding of their extracellular domains but also transmit signals into the cell to initiate a response to the change in its surroundings. The activity of many adhesion receptors can be regulated by intracellular signals via an apparent inside-out pathway. While the molecular mechanisms underlying the outside-in and inside-out signaling pathways have been the target of numerous studies, most of which are concentrated on platelet-specific integrin αIIbβ3,[1−3] general principles for the adhesion receptor-mediated transmembrane signaling remain to be elucidated.

The glycoprotein Ib-IX (GPIb-IX) complex is expressed in the plasma membrane of platelets and plays a critical role in the initiation of thrombosis and hemostasis. This adhesion receptor complex consists of three type I transmembrane protein subunits, GPIbα, GPIbβ, and GPIX, with a 1:2:1 stoichiometry.[4,5] GPIbα connects with two GPIbβ subunits through membrane-proximal disulfide bonds to form a complex called GPIb.[5] GPIX is tightly associated with GPIb through noncovalent forces in both extracellular and transmembrane domains.[4,6−8] In the GPIb-IX complex, the N-terminal leucine-rich repeat domain of GPIbα contains the binding site for its physiological ligand, VWF.[9−11] Upon ligation with the A1 domain of VWF, the GPIb-IX complex transmits inwardly, through the cytoplasmic tail of GPIbα, an activating signal that leads to activation of integrin αIIbβ3 and eventual platelet aggregation.[12,13] A recent study shows that although mouse platelets expressing a PT-VWD mutation in the N-terminal ligand-binding domain of GPIbα spontaneously bind to VWF

Received: August 25, 2011
Revised: November 10, 2011
Published: November 14, 2011

as expected, the platelets were surprisingly inactive and failed to respond to agonist treatment, suggesting that the mutant GPIb-IX complex transmits an inhibitory signal into the platelet.[14] In addition to mediating outside-in signaling events, the GPIb-IX complex undergoes inside-out regulation. For instance, a change in the phosphorylation state of Ser166 in the cytoplasmic domain of GPIbβ can influence binding of VWF to the N-terminal domain of GPIbα.[15,16] Moreover, a 27 bp deletion in the macroglycopeptide-coding region of the GPIBA gene has been identified in certain PT-VWD patients.[17] The deletion, distal to the ligand-binding domain but proximal to the transmembrane domain of GPIbα, increased the VWF binding function of GPIbα that is heterologously expressed in mammalian cells.[17] However, our understanding of the mechanism by which the GPIb-IX complex transmits signals in both directions remains limited, partly because of the difficulty in characterizing multisubunit membrane protein complexes and the lack of a suitable in vitro experimental system for this complex.

Phospholipid bilayer Nanodiscs are novel model membranes derived from nascent discoidal high-density lipoprotein particles.[18,19] One disk contains a patch of phospholipid, which is wrapped by two copies of membrane scaffold protein (MSP) derived from human apolipoprotein A-I.[19] Because of the presence of the protein coat MSP, Nanodiscs are soluble and monodisperse and have well-defined diameters, ranging from 9.4 to 12 nm depending on the size of MSP.[19,20] Therefore, the membrane proteins placed into the Nanodisc have the "native-like" membrane environment. The exposure of both extracellular and intracellular domains of a membrane protein to the same aqueous environment is particularly amenable to spectroscopic investigation. Indeed, Nanodiscs have been adopted in studies of a variety of membrane proteins, including bacteriorhodopsin and G protein-coupled receptors,[21−23] bacterial chemoreceptors,[24] epidermal growth factor receptor (EGFR),[25] and integrin αIIbβ3.[26]

We have incorporated the platelet GPIb-IX complex into the phospholipid bilayer Nanodiscs. The GPIb-IX complex adopts the native-like conformation in Nanodiscs and is capable of binding to VWF with subnanomolar binding affinity. An in vitro experimental platform has therefore been established for future investigation of the mechanism of signal transmission through the GPIb-IX complex.

MATERIALS AND METHODS

Reagents and Antibodies. POPC was obtained from Avanti Polar Lipids (Alabaster, AL). Monoclonal antibodies against individual subunits of the GPIb-IX complex, including WM23, SZ2, AN51, FMC25, AK2, and Gi27, were either obtained from the hybridoma cell line or purchased from Beckman Coulter (Fullerton, CA), Dako (Carpinteria, CA), Millipore (Billerica, MA), AbD Serotec (Raleigh, NC), or Chemicon (Temecula, CA). Mouse and rat IgG and HRP-conjugated secondary antibodies were purchased from Santa Cruz Biotechnology (Santa Cruz, CA). Human VWF and botrocetin were obtained from American Diagnostica Inc. (Greenwich, CT) and Centerchem Inc. (Norwalk, CT), respectively. Bovine pancreas DNase I was from Roche Applied Science (Indianapolis, IN). The MSP1D1 plasmid was obtained from Addgene (Cambridge, MA). Monoclonal antibody RAM.1 and the A1A2A3 fragment of VWF were obtained as previously described.[27,28]

Purification of the Human Platelet GPIb-IX Complex. Purification of the platelet GPIb-IX complex followed published protocols[29,30] with some modifications. Four units of fresh concentrated PRP were obtained from the Gulf Coast Regional Blood Center (Houston, TX), from which platelets were pelleted in the presence of 5 mM EDTA at 1300*g* and room temperature for 10 min and washed once with CGS buffer [120 mM NaCl, 30 mM D-glucose, and 12.9 mM trisodium citrate (pH 6.5)] containing 5 mM EDTA. Pelleted platelets were resuspended in buffer A [20 mM Tris-HCl, 150 mM NaCl, and 10 mM EDTA (pH 7.4)] with 200 mM sucrose, a 1:50 (v/v) dilution of protease inhibitor cocktail (Sigma, St. Louis, MO), and 1 mM PMSF (Amresco, Solon, OH) and sonicated with a Branson (Danbury, CT) Sonifier 250 until the suspension became clear. The platelet membrane portion was extracted from the lysate by centrifugation at 180000*g* and 4 °C for 1 h and then dissolved in ice-cold buffer A containing 1% Triton X-100, 5 mM *N*-ethylmaleimide (Sigma), a 1:50 dilution of protease inhibitor cocktail, and 1 mM PMSF at 4 °C for 2 h. The Triton X-100-soluble fraction was isolated by centrifugation at 180000*g* and 4 °C for 3 h to remove the cytoskeleton.

The soluble fraction was incubated with 2 mg/mL DNase I on ice for 1.5 h to depolymerize any remaining actin filaments and then applied to a wheat germ agglutinin (WGA) column (Calbiochem, San Diego, CA). The column was washed thoroughly with buffer B [20 mM Tris-HCl, 150 mM NaCl, 1 mM EDTA, and 0.1% Triton X-100 (pH 7.4)], and the bound proteins were eluted with buffer B containing 2.5% *N*-acetyl-D-glucosamine (Sigma). The eluent was further purified via anion exchange chromatography (Resource Q column, GE Healthcare, Piscataway, NJ) using a linear gradient from 0.15 to 1 M NaCl in 20 mM Tris-HCl, 1 mM EDTA, and 0.1% Triton X-100 (pH 7.4). The eluted GPIb-IX complex was concentrated and changed to buffer B using Amicon Ultra 15 mL filters with a 10 kDa molecular mass cutoff (Millipore) before being stored at −80 °C. The concentration of the GPIb-IX complex was determined using a BCA protein assay kit (Pierce Biotechnology, Rockford, IL).

Purification of Platelet Glycocalicin. Glycocalicin, also known as the soluble extracellular domain of GPIbα, was isolated from human platelets by a variation of an earlier method.[31] Briefly, platelets were pelleted from 3 units of fresh PRP at 1300*g* for 10 min at room temperature. The pelleted platelets were washed once with CGS buffer, resuspended in 40 mL of TBS buffer [20 mM Tris-HCl and 100 mM NaCl (pH 7.4)] containing 2 mM $CaCl_2$, and sonicated to lyse the cells. The mixture was then incubated at 37 °C for 1 h to allow the proteolytic cleavage of GPIbα to generate glycocalicin. PMSF (1 mM) and EDTA (5 mM) were added to quench further proteolysis after the incubation. After ultracentrifugation at 80000*g* and 4 °C for 1 h to remove cell components, the glycocalicin-containing supernatant was applied to a WGA column. After being washed with TBS buffer, the bound proteins were eluted with elution buffer [20 mM Tris-HCl and 2.5% *N*-actyl-D-glucosamine (pH 7.4)]. The eluent was further loaded onto a Resource Q column with a linear gradient from 0 to 1 M NaCl in 20 mM Tris-HCl (pH 7.4) over 40 mL. Glycocalicin was further purified through a Superose 6 10/300 GL gel filtration column (GE Healthcare).

Reconstitution of the GPIb-IX Complex in Nanodiscs. MSP1D1 was expressed in *Escherichia coli* BL21(DE3) cells and purified by Ni affinity chromatography following the published protocol.[18] POPC dissolved in chloroform was dried in a glass

vial by a gentle argon stream to a thin film and placed under vacuum overnight to remove residual solvent. The dried lipid was hydrated with hydration buffer [20 mM Tris-HCl, 100 mM NaCl, 100 mM sodium cholate, and 0.01% NaN_3 (pH 7.4)] to a final concentration of 50 mM.

Empty Nanodiscs and GPIb-IX complex-containing Nanodiscs (GPIb-IX/ND) were assembled according to the published protocols.[25,32] Briefly, 300 μL of assembly reaction mixture containing 1 mM POPC, 25 μM MSP1D1, and 16 mM sodium cholate without or with 1 μM GPIb-IX complex was incubated at room temperature for 45 min and then placed on ice for 1 h. The assembly of Nanodiscs was initiated with the addition of 0.15 g (empty Nanodiscs) or 0.24 g (GPIb-IX/ND) of damp Biobeads SM-2 (Bio-Rad, Richmond, CA), and the reaction complex was gently rocked at 4 °C for 16 h. After assembly, the Biobeads were removed by centrifugation at 10000*g* for 1 min and the supernatant was applied to a Superose 6 10/300 GL column (GE Healthcare) calibrated by molecular mass standards (Bio-Rad) to analyze the mixture and to purify assembled Nanodiscs.

ELISA. Nanodiscs (~4 μg/mL) or 1% BSA (R&D Systems, Minneapolis, MN) was immobilized onto a microtiter plate at 4 °C overnight, and the wells were blocked with 1% BSA in PBS. To probe the conformation of the GPIb-IX complex, conformation-sensitive monoclonal antibodies against various components of the GPIb-IX complex were added to Nanodisc- or BSA-coated wells followed by either HRP-conjugated goat anti-mouse IgG or goat anti-rat IgG. To assess binding of VWF, we added various concentrations of VWF with 0.2 unit/mL botrocetin, followed by rabbit anti-VWF antibody (2 μg/mL) and HRP-conjugated goat anti-rabbit IgG (1:5000). The incubation was conducted at room temperature for 1 h unless specifically stated, and wells were washed four times with PBS between every two steps. After incubation of antibodies and standard washing, substrate tetramethylbenzidine (R&D Systems) was added to each well, and the plates were incubated for 20 min. The reaction was stopped by addition of 25 μL of 1 M H_2SO_4 to each well, and the plate was read at 450 nm (with wavelength correction at 570 nm) in a Dynex MRX ELISA plate reader (Dynex Technologies, Chantilly, VA).

To compare the ligand binding function of the GPIb-IX complex versus that of glycocalicin, 4 μg/mL WM23 in PBS was first immobilized in the microtiter wells at 4 °C overnight. After the wells had been blocked with 1% BSA in PBS, GPIb-IX/ND, glycocalicin, empty Nanodiscs, and 4 μg/mL BSA were added to the wells. After capture, full-length VWF or A1A2A3 domains with 0.2 unit/mL botrocetin were incubated, and the binding was detected with rabbit anti-VWF antibody and HRP-conjugated goat anti-rabbit antibody. To compare the efficiency of capture, the WM23 $F(ab')_2$ fragment was generated using the mouse IgG $F(ab')_2$ fragment preparation kit (Pierce Biotechnology) and used to coat the wells. The anti-GPIbα monoclonal antibody and HRP-conjugated goat anti-mouse IgG Fc (Pierce Biotechnology) were used to detect captured GPIb-IX/ND and glycocalicin.

After the background signal had been subtracted, the binding curve was fitted to the equation

$$Y = B_{max} \times x/(K_d + x)$$

where Y is the specific binding, x the ligand concentration, B_{max} the binding maximum, and K_d the equilibrium dissociation constant.

Electron Microscopy of Nanodiscs. Purified GPIb-IX/ND [~10 μg/mL in 20 mM Tris-HCl (pH 7.4)] was applied to a copper EM grid containing a carbon film support. The specimen was stained with 0.7% uranyl acetate. Images were taken on a model JEM-1200 EX transmission electron microscope (JEOL, Peabody, MA) at a magnification of 40000× and recorded on a TVIPS F215 2K × 2K CCD camera (TVIPS, Gauting, Germany).

RESULTS

Assembly of the Platelet GPIb-IX Complex into Phospholipid Nanodiscs. The GPIb-IX complex was purified from human platelet concentrates. Figure 1A shows

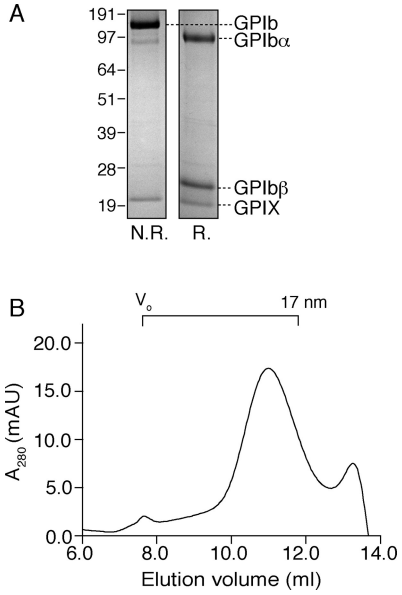

Figure 1. Characterization of the purified GPIb-IX complex in Triton X-100. (A) The GPIb-IX complex was purified from human platelets and solubilized in 0.1% Triton X-100-containing buffer. The complex was resolved in a 10% SDS gel under both nonreducing (N.R.) and reducing (R.) conditions and detected by Coomassie blue staining. (B) The purified GPIb-IX complex was applied to a Superose 6 gel filtration column equilibrated with 0.1% Triton X-100-containing buffer. Protein elution was monitored by the absorbance at 280 nm (A_{280}). The calibrated Stokes diameter scale and void volume for this column are shown at the top.

the sodium dodecyl sulfate−polyacrylamide gel electrophoresis profile of the purified GPIb-IX complex. Under nonreducing conditions, GPIb and GPIX bands were present in the SDS gel, constituting more than 95% of the detectable protein. Under reducing conditions, GPIb dissociates into GPIbα and GPIbβ subunits.[4,5] To determine the size of the complex before it assembles into Nanodiscs, the purified GPIb-IX complex in the Triton X-100-containing buffer was analyzed by gel filtration chromatography (Figure 1B). Partly because of the elongated shape of GPIbα,[33] the complex was eluted with a Stokes diameter of approximately 24 nm.

Empty Nanodiscs were first assembled using POPC and MSP1D1. The POPC:MSP1D1 molar ratio was optimized to minimize protein aggregation and maximize Nanodisc assembly. As shown in Figure 2A, empty Nanodiscs were eluted with a Stokes diameter of approximately 9.5 nm from the gel filtration column, consistent with a Stokes diameter of 9.5 nm for Nanodiscs comprising MSP1D1 and DMPC[20] and 9.6

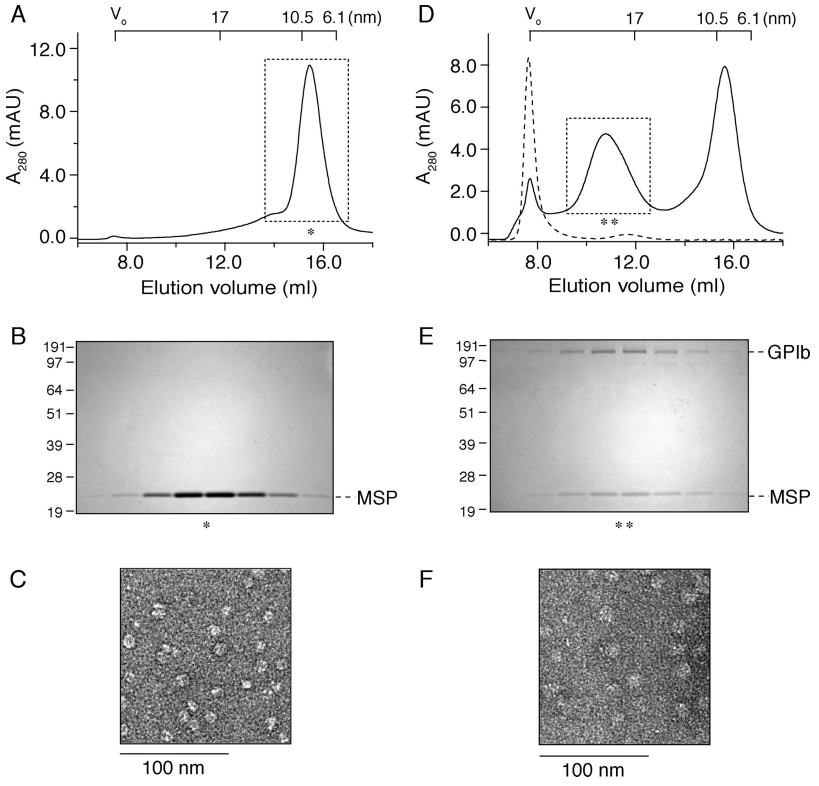

Figure 2. Assembly of the purified platelet GPIb-IX complex into phospholipid bilayer Nanodiscs. (A) Empty Nanodiscs were assembled with the optimized ratio of POPC to MSP1D1 and separated by the Superose 6 gel filtration column. (B) The fractions from the peak (asterisk) in panel A were resolved in a 10% SDS gel under nonreducing conditions and stained with Coomassie blue. (D) The GPIb-IX complex was incorporated into excess Nanodiscs and purified with a Superose 6 column (solid line); the GPIb-IX complex was mixed only with POPC and analyzed with a Superose 6 column (dashed line). (E) The fractions from the peak (two asterisks) in panel D were resolved in a 10% SDS gel under nonreducing conditions and stained with Coomassie blue. Elution of Nanodiscs was monitored by the absorbance at 280 nm (A_{280}). The calibrated Stokes diameter scale and void volume for this column are shown atop panels A and D. Negative-stain TEM of empty Nanodiscs (C) and Nanodiscs with the GPIb-IX complex (F) with a magnification of 40000×. The scale bars are shown below the images.

nm for those comprising MSP1D1 and egg PC.[25] Visualization of MSP1D1 in a SDS gel shown in Figure 2B and the TEM image of empty Nanodiscs in Figure 2C confirmed the success of the assembly.

To assemble the GPIb-IX complex into Nanodiscs, the GPIb-IX complex solubilized in 0.1% Triton X-100 was mixed with excess MSP1D1 and POPC so that at most one copy of the complex was reconstituted into a Nanodisc. After removal of the detergent by Biobeads, the mixture was analyzed by gel filtration chromatography. In addition to the peak of empty Nanodiscs, another well-separated peak with an apparent Stokes diameter of approximately 27 nm was observed (Figure 2D). This peak contained GPIb-IX complex-embedded Nanodiscs (GPIb-IX/ND), because GPIb and MSP1D1 were co-eluted from the column (Figure 2E). The presence of both GPIbα and GPIX in the disks was further confirmed by an ELISA (Figure 3). The Stokes diameter of GPIb-IX/ND is slightly larger than that of the GPIb-IX complex in Triton X-100-containing buffer, consistent with the expectation that a Nanodisc is larger than a detergent micelle. The TEM image shows the disk shape density, further confirming the success of assembly (Figure 2F). As a negative control, the GPIb-IX complex was mixed with POPC but without MSP, and it was eluted at the void volume (Figure 2D), indicating that the complex was reconstituted into POPC lipid vesicles or formed large aggregates during the process.

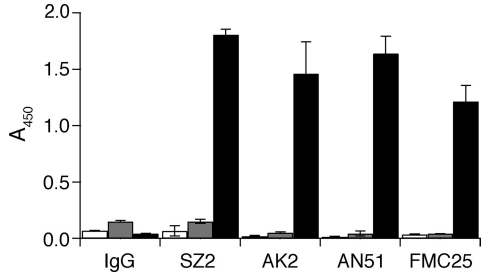

Figure 3. Probing the GPIb-IX complex reconstituted in Nanodiscs by conformation-sensitive monoclonal antibodies. Mouse IgG (1 μg/mL) or antibodies against GPIbα (SZ2, AK2, and AN51) or GPIX (FMC25) were incubated with immobilized GPIb-IX/ND (black), empty Nanodiscs (gray), or BSA (white). The bound antibodies were detected by an ELISA, using HRP-conjugated goat anti-mouse antibody. The absorbance at 450 nm was measured in three independent experiments and is presented as the mean ± the standard deviation.

To determine the stoichiometry of GPIb-IX complex-containing Nanodiscs, intensities of GPIb and MSP1D1 protein bands in Figure 2E were compared and the molar ratio of GPIb to MSP1D1 was calculated to approximately 0.4:1 on the basis of calibration of the difference between the Coomassie blue staining efficiency of GPIb and MSP1D1 in SDS gels (Figure S1 of the Supporting Information). Because there are two copies of MSP1D1 per disk, our results suggested that only one

dx.doi.org/10.1021/bi201351d | *Biochemistry* 2011, 50, 10598–10606

copy of the GPIb-IX complex was incorporated into a Nanodisc.

VWF Binding Function of the GPIb-IX Complex Reconstituted in Nanodiscs. To evaluate the quality of the GPIb-IX complex reconstituted in Nanodiscs, we first probed the conformation of GPIbα and GPIX using conformation-sensitive monoclonal antibodies. SZ2, AN51, and AK2 recognize distinct three-dimensional epitopes in or around the N-terminal ligand-binding domain of GPIbα,[34,35] whereas FMC25 recognizes only the well-folded GPIX ectodomain.[30] GPIb-IX/ND, empty Nanodiscs, or BSA was directly coated on the walls of microtiter wells and antibody binding detected with an ELISA with HRP-conjugated secondary antibody. As shown in Figure 3, all the monoclonal antibodies tested bound to wells coated with GPIb-IX/ND but not to those with empty Nanodisc or BSA, indicating that the GPIb-IX complex reconstituted in Nanodiscs adopts the native-like conformation. Moreover, the conformation of GPIb-IX/ND is stable as it retains binding to conformation-sensitive antibodies after being stored at 4 °C for 2 weeks (data not shown).

Next we determined the affinity of VWF for GPIb-IX/ND in the presence of botrocetin, which mediates the interaction between GPIbα and VWF under static conditions.[36] Because it is more difficult to accurately measure the concentration of GPIb-IX/ND than that of VWF, GPIb-IX/ND was immobilized in the ELISA and the amount of bound VWF in the microtiter well was measured using anti-VWF antibody. Figure 4A shows that VWF bound to GPIb-IX/ND in a concentration-dependent and saturable manner, with an apparent dissociation constant of 0.73 ± 0.07 nM if the molar concentration of VWF was calculated with a molecular mass of 250 kDa. The measured dissociation constant is the same as that observed for fixed human platelets (data not shown) and comparable with those from previous reports.[37,38] The effects of antibodies against each subunit of the GPIb-IX complex on VWF binding were also tested. AK2, targeting the ligand-binding domain of GPIbα,[34] abolished botrocetin-induced VWF binding, indicating that the binding is specific to GPIbα. As expected, FMC25, targeting the GPIX extracellular domain, or Gi27, targeting the GPIbβ cytoplasmic domain, had no effect (Figure 4B). Overall, these results showed that the GPIb-IX complex retains its normal ligand binding function when reconstituted in Nanodiscs.

Effect of RAM.1 on Binding of VWF to the GPIb-IX Complex in Nanodiscs. Although the binding site for VWF is located on the N-terminus of GPIbα, GPIbβ has been shown to regulate the ligand binding function of GPIbα, either through their cytoplasmic tails[15,16] or through the membrane-proximal disulfide bonds.[39] RAM.1, a rat monoclonal antibody that recognizes the extracellular part (Cys68−Cys93) of GPIbβ, hampers botrocetin-induced binding of platelets or GPIb-IX complex-transfected cells to VWF as well as their adhesion to VWF under flow conditions.[27,40] We tested whether RAM.1 can hamper the association of GPIb-IX/ND with VWF in vitro. As shown in Figure 5A, RAM.1 bound to GPIb-IX/ND, but not to empty Nanodiscs or BSA that were immobilized in microtiter wells. However, after 10 μg/mL rat IgG or RAM.1 was preincubated with immobilized GPIb-IX/ND, no significant difference in botrocetin-mediated VWF binding was observed (Figure 5B). Similar results were observed when a higher concentration of RAM.1 was used in preincubation, when GPIb-IX/ND was captured by WM23 instead of being

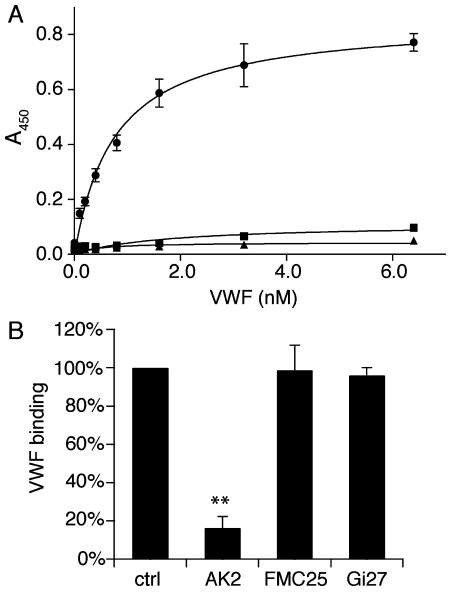

Figure 4. Botrocetin-induced binding of VWF to the GPIb-IX complex reconstituted in Nanodiscs. (A) Botrocetin-induced binding of VWF to the GPIb-IX complex in Nanodiscs measured with an ELISA. Increasing concentrations of VWF were incubated with immobilized GPIb-IX/ND (●), empty Nanodiscs (■), or BSA (▲) in the presence of 0.2 unit/mL botrocetin. The binding of VWF was assessed with rabbit anti-VWF antibody and HRP-conjugated goat anti-rabbit antibody. (B) Effect of monoclonal antibodies against individual subunits of the GPIb-IX complex on VWF binding. Antibodies (10 μg/mL) were preincubated with immobilized GPIb-IX/ND before 0.8 nM VWF with 0.2 unit/mL botrocetin was added. The bound VWF was detected by HRP-conjugated anti-VWF antibody. The absorbance at 450 nm was measured in three independent experiments and is presented as the mean ± the standard deviation. For some data points, the error bars are smaller than the symbols. One hundred percent in panel B is defined as the binding of VWF to GPIb-IX/ND in the absence of inhibitory antibodies after subtraction of the binding to empty Nanodiscs. Groups were compared using the Student's t test. $^{**}P < 0.01$ vs control.

coated directly onto microtiter wells, or when recombinant A1A2A3 tridomains of VWF were used for binding. Thus, these results suggest that the effect of RAM.1 on VWF binding observed in platelets or GPIb-IX complex-transfected cells may not be due to direct interference with the VWF−GPIbα interaction and thus is unlikely to be restricted to the extracellular domain of GPIbβ.

Comparison of Ligand Binding between GPIb-IX/ND and Glycocalicin. To further investigate the role of GPIbβ in the ligand binding function of GPIbα, binding of full-length VWF or A1A2A3 tridomains to GPIb-IX/ND in the presence of botrocetin was compared to binding to glycocalicin by an ELISA. Because glycocalicin could not be recognized by AN51 when it was directly coated to microtiter wells, WM23, a mouse monoclonal antibody targeting the macroglycopeptide portion of GPIbα, was used to capture GPIb-IX/ND and glycocalicin in microtiter wells. Although results of an ELISA showed that apparent dissociation constants obtained for interaction with full-length VWF or A1A2A3 tridomains were indistinguishable between GPIb-IX/ND and glycocalicin, the amount of bound VWF or A1A2A3 was different for GPIb-IX/ND and glycocalicin (Figure 6A,B). To explain this difference, SZ2, a monoclonal antibody targeting the N-terminal domain of GPIbα, was used to detect the amount of GPIb-IX/ND and

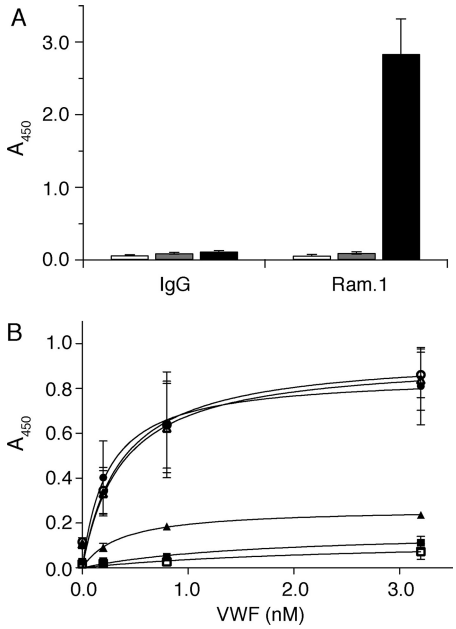

Figure 5. Effect of RAM.1 on the VWF binding activity of the GPIb-IX complex reconstituted in Nanodiscs. (A) Binding of RAM.1 to the GPIb-IX complex in Nanodiscs. Rat IgG or RAM.1 (each at 2 μg/mL) was incubated with immobilized GPIb-IX/ND (black) or empty Nanodiscs (gray), or BSA (white), and the binding was detected by HRP-conjugated goat anti-rat antibody. (B) Effect of RAM.1 on botrocetin-induced binding of VWF to the GPIb-IX complex in Nanodiscs. Antibodies at 10 μg/mL, rat IgG (○) and RAM.1 (●), mouse IgG (△), and AK2 (▲), were preincubated with GPIb-IX/ND-coated wells, and then increasing concentrations of VWF with 0.2 unit/mL botrocetin was added. The binding was detected by HRP-conjugated anti-VWF antibody. The addition of VWF with botrocetin to empty Nanodisc-coated (■) or BSA-coated (□) wells served as a negative control. The absorbance at 450 nm was measured in three independent experiments and is presented as the mean ± the standard deviation. For some data points, the error bars are smaller than the symbols.

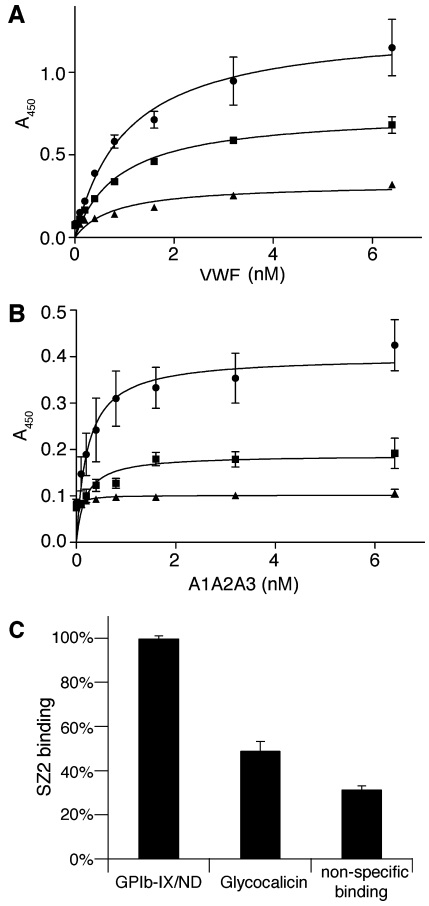

Figure 6. Comparison of ligand binding activities between GPIb-IX/ND and glycocalicin. WM23 IgG (4 μg/mL) was immobilized onto microtiter wells to capture GPIb-IX/ND (●) and glycocalicin (■). Empty Nanodiscs (▲) were also added to the WM23-coated wells as a control. (A) Full-length VWF (0−6.4 nM) or (B) A1A2A3 tridomains (0−6.4 nM) were incubated with GPIb-IX/ND, glycocalicin, or control wells in the presence of 0.2 unit/mL botrocetin. The binding was detected by anti-VWF antibody and HRP-conjugated secondary antibody. (C) Difference in capturing efficiency. The WM23 IgG $F(ab')_2$ fragment (4 μg/mL) was coated to microtiter wells to capture GPIb-IX/ND or glycocalicin. Empty Nanodiscs were also added to the wells coated with the WM23 $F(ab')_2$ fragment as a control. SZ2 (1 μg/mL) was incubated and detected by HRP-conjugated goat anti-mouse antibody. "Nonspecific binding" is the binding of SZ2 to the control wells. The absorbance at 450 nm was measured in three independent experiments and is presented as the mean ± the standard deviation. For some of the points, the error bars are smaller than the symbols. One hundred percent in panel C is defined as the binding of SZ2 to GPIb-IX/ND captured by the WM23 $F(ab')_2$ fragment.

glycocalicin immobilized by the WM23 $F(ab')_2$ fragment in microtiter wells. As shown in Figure 6C, significantly more GPIb-IX/ND than glycocalicin was present in the well, although the same amount of the WM23 $F(ab')_2$ fragment was used for immobilization. Moreover, the difference in WM23's capturing abilities between GPIb-IX/ND and glycocalicin matches the difference in bound A1A2A3 tridomains in ELISAs, indicating that the apparent weaker binding of A1A2A3 to glycocalicin is due to the lower capture efficiency of glycocalicin by WM23 (Figure 6B). Because full-length VWF is multimeric, the amount of bound VWF may not be simply correlated with that of the captured receptor. Thus, there appeared to be little difference in the ligand binding function between the GPIb-IX complex reconstituted in Nanodiscs and glycocalicin in the presence of botrocetin.

■ DISCUSSION

Compared to detergent micelles, Nanodiscs provide membrane proteins with a real phospholipid bilayer environment that mimics the cell membrane. Phosphatidylcholine, the most abundant phospholipid in cell membranes, was used in this study to construct the Nanodisc. Compared to phospholipid vesicles, Nanodiscs also offer several advantages.[19] One of the advantages is the simultaneous access to both extracellular and cytoplasmic domains of the membrane receptor embedded in Nanodiscs. This is particularly useful for mechanistic studies of receptor-mediated signal transduction across the membrane.[24,26] Thus, reconstitution of the functional GPIb-IX complex into phospholipid Nanodiscs will provide a useful platform for mechanistic investigations of GPIb-IX complex-mediated transmembrane signaling events.

In this study, we have reconstituted the purified GPIb-IX complex into phospholipid Nanodiscs and shown that the GPIb-IX complex is functional in this novel model membrane. Incorporation of the GPIb-IX complex into Nanodiscs was confirmed by three lines of evidence. First, MSP1D1 co-eluted

with GPIb from the gel filtration column after assembly. Co-elution of 25 kDa MSP1D1 with 220 kDa GPIb-IX complex indicates that they are bound together and eluted as a complex. Second, GPIb-IX/ND eluted at a slightly larger Stokes diameter than the GPIb-IX complex dissolved in the Triton X-100-containing buffer. The average molecular mass of a Triton X-100 micelle is 80 kDa.[41] Assuming that there are 160 molecules of POPC in each Nanodisc, the molecular mass of one empty disk is 170 kDa.[20] The higher molecular mass of a disk compared to a detergent micelle would explain the slightly larger Stokes diameter of GPIb-IX/ND. A similar difference was also observed for EGFR reconstituted in Nanodiscs versus that dissolved in the Triton X-100-containing buffer.[26] Finally, the negative-stain TEM image of GPIb-IX/ND showed the disk shape density, consistent with previous reports.[42]

Reconstituted in the Nanodisc, the GPIb-IX complex adopts the native conformation as it is able to bind all the conformation-sensitive antibodies tested in this study. The GPIb-IX complex in Nanodiscs is stable for at least 2 weeks (data not shown). Moreover, it shows native-like ligand binding properties, having exhibited the same binding affinity for VWF in the presence of botrocetin as in previous reports.[37,38] The binding affinity measured in this study is also comparable to those previously reported for the binding of the N-terminal fragment of GPIbα to VWF in the presence of botrocetin.[11,43]

GPIbβ plays a central role in assembly of the GPIb-IX complex. It interacts with GPIbα through a disulfide bond near the membrane as well as interactions between their transmembrane domain.[5,44,45] There is also cross-talk between the cytoplasmic tails of these two subunits through the association with 14-3-3ζ.[15] In a related manner, binding of RAM.1 antibody to the GPIbβ extracellular domain leads to the alteration of the cytoplasmic tails of GPIb and at the same time hampers the ligand binding ability of the extracellular domain of GPIbα.[40] The molecular mechanism underlying GPIbβ modulation of the VWF binding function of GPIbα is not clear. One possible mechanism may be that the GPIbβ extracellular domain, with or without RAM.1, directly participates in an interaction with VWF and thus directly modulates the GPIbα–VWF interaction. To test this possibility, we compared binding of VWF to glycocalicin versus GPIb-IX/ND. Consistent with a previous study,[38] although glycocalicin and GPIb-IX/ND for some reason exhibit different immobilization efficiencies with WM23, little difference in binding affinity was observed (Figure 6). Furthermore, while RAM.1 exhibited specific binding to GPIb-IX/ND, it did not have any detectable effect on the association of VWF with GPIb-IX/ND in the presence of botrocetin (Figure 5). These results indicate that the GPIbβ extracellular domain may not directly participate in the interaction with VWF or modulate the GPIbα–VWF interaction, and that the observed effects of RAM.1 on VWF binding by platelets and GPIb-IX complex-expressing cells may require other factors inside the cell. One possible scenario is that RAM.1 binding to the GPIbβ extracellular domain may transmit a signal into the platelet, through perhaps association of 14-3-3ζ with cytoplasmic domains of the GPIb-IX complex,[15,16,46−48] and influence the surface distribution and/or the overall binding activity of the GPIb-IX complex. Further investigation will be needed to elucidate the apparent trans-subunit effects of RAM.1 on GPIb-IX complex function and signaling.

■ ASSOCIATED CONTENT

Supporting Information

Calibration of GPIb and MSP staining in SDS gels. This material is available free of charge via the Internet at http://pubs.acs.org.

■ AUTHOR INFORMATION

Corresponding Author

*Aflac Cancer Center and Blood Disorders Service, 2015 Uppergate Dr., Room 426A, Atlanta, GA 30322. Telephone: (404) 727-8217. Fax: (404) 727-4859. E-mail: renhao.li@emory.edu.

Funding

Supported by National Institutes of Health Grant HL082808.

■ ACKNOWLEDGMENTS

We thank Ms. Katie Sowa and Limei H. Jones for technical assistance.

■ ABBREVIATIONS

PT-VWD, platelet-type von Willebrand disease; POPC, 1-palmitoyl-2-oleoyl-*sn*-glycero-3-phosphocholine; HRP, horseradish peroxidase; PRP, platelet-rich plasma; PMSF, phenylmethanesulfonyl fluoride; ELISA, enzyme-linked immunosorbent assay; BSA, bovine serum albumin; TEM, transmission electron microscopy.

■ REFERENCES

(1) Takagi, J., Petre, B. M., Walz, T., and Springer, T. A. (2002) Global conformational rearrangements in integrin extracellular domains in outside-in and inside-out signaling. *Cell 110*, 599−611.

(2) Vinogradova, O., Velyvis, A., Velyviene, A., Hu, B., Haas, T. A., Plow, E. F., and Qin, J. (2002) A structural mechanism of integrin αIIbβ3 "inside-out" activation as regulated by its cytoplasmic face. *Cell 110*, 587−597.

(3) O'Toole, T. E., Mandelman, D., Forsyth, J., Shattil, S. J., Plow, E. F., and Ginsberg, M. H. (1991) Modulation of the affinity of integrin αIIbβ3 (GPIIb-IIIa) by the cytoplasmic domain of αIIb. *Science 254*, 845−847.

(4) Du, X., Beutler, L., Ruan, C., Castaldi, P. A., and Berndt, M. C. (1987) Glycoprotein Ib and glycoprotein IX are fully complexed in the intact platelet membrane. *Blood 69*, 1524−1527.

(5) Luo, S.-Z., Mo, X., Afshar-Kharghan, V., Srinivasan, S., Lopez, J. A., and Li, R. (2007) Glycoprotein Ibα forms disulfide bonds with 2 glycoprotein Ibβ subunits in the resting platelet. *Blood 109*, 603−609.

(6) Luo, S.-Z., Mo, X., López, J. A., and Li, R. (2007) Role of the transmembrane domain of glycoprotein IX in assembly of the glycoprotein Ib-IX complex. *J. Thromb. Haemostasis 5*, 2494−2502.

(7) Mo, X., Nguyen, N. X., McEwan, P. A., Zheng, X., Lopez, J. A., Emsley, J., and Li, R. (2009) Binding of platelet glycoprotein Ibβ through the convex surface of leucine-rich repeats domain of glycoprotein IX. *J. Thromb. Haemostasis 7*, 1533−1540.

(8) McEwan, P. A., Yang, W., Carr, K. H., Mo, X., Zheng, X., Li, R., and Emsley, J. (2011) Quaternary organization of GPIb-IX complex and insights into Bernard-Soulier syndrome revealed by the structures of GPIbβ and a GPIbβ/GPIX chimera. *Blood 118*, 5292−5301.

(9) Huizinga, E. G., Tsuji, S., Romijn, R. A., Schiphorst, M. E., de Groot, P. G., Sixma, J. J., and Gros, P. (2002) Structures of glycoprotein Ibα and its complex with von Willebrand factor A1 domain. *Science 297*, 1176−1179.

(10) Cauwenberghs, N., Vanhoorelbeke, K., Vauterin, S., and Deckmyn, H. (2000) Structural determinants within platelet glycoprotein Ibα involved in its binding to von Willebrand factor. *Platelets 11*, 373−378.

(11) Miura, S., Li, C. Q., Cao, Z., Wang, H., Wardell, M. R., and Sadler, J. E. (2000) Interaction of von Willebrand factor domain A1 with platelet glycoprotein Ibα-(1−289). Slow intrinsic binding kinetics mediate rapid platelet adhesion. *J. Biol. Chem. 275*, 7539−7546.
(12) Kroll, M. H., Harris, T. S., Moake, J. L., Handin, R. I., and Schafer, A. I. (1991) von Willebrand factor binding to platelet GpIb initiates signals for platelet activation. *J. Clin. Invest. 88*, 1568−1573.
(13) Savage, B., Shattil, S. J., and Ruggeri, Z. M. (1992) Modulation of platelet function through adhesion receptors. A dual role for glycoprotein IIb-IIIa (integrin αIIbβ3) mediated by fibrinogen and glycoprotein Ib-von Willebrand factor. *J. Biol. Chem. 267*, 11300−11306.
(14) Guerrero, J. A., Kyei, M., Russell, S., Liu, J., Gartner, T. K., Storrie, B., and Ware, J. (2009) Visualizing the von Willebrand factor/glycoprotein Ib-IX axis with a platelet-type von Willebrand disease mutation. *Blood 114*, 5541−5546.
(15) Dai, K., Bodnar, R., Berndt, M. C., and Du, X. (2005) A critical role for 14-3-3ζ protein in regulating the VWF binding function of platelet glycoprotein Ib-IX and its therapeutic implications. *Blood 106*, 1975−1981.
(16) Bodnar, R. J., Xi, X., Li, Z., Berndt, M. C., and Du, X. (2002) Regulation of glycoprotein Ib-IX-von Willebrand factor interaction by cAMP-dependent protein kinase-mediated phosphorylation at Ser 166 of glycoprotein Ibβ. *J. Biol. Chem. 277*, 47080−47087.
(17) Othman, M., Notley, C., Lavender, F. L., White, H., Byrne, C. D., Lillicrap, D., and O'Shaughnessy, D. F. (2005) Identification and functional characterization of a novel 27-bp deletion in the macroglycopeptide-coding region of the GPIbα gene resulting in platelet-type von Willebrand disease. *Blood 105*, 4330−4336.
(18) Bayburt, T. H., Grinkova, Y. V., and Sligar, S. G. (2002) self-assembly of discoidal phospholipid bilayer nanoparticles with membrane scaffold proteins. *Nano Lett. 2*, 853−856.
(19) Nath, A., Atkins, W. M., and Sligar, S. G. (2007) Applications of phospholipid bilayer nanodiscs in the study of membranes and membrane proteins. *Biochemistry 46*, 2059−2069.
(20) Denisov, I. G., Grinkova, Y. V., Lazarides, A. A., and Sligar, S. G. (2004) Directed self-assembly of monodisperse phospholipid bilayer Nanodiscs with controlled size. *J. Am. Chem. Soc. 126*, 3477−3487.
(21) Bayburt, T. H., Grinkova, Y. V., and Sligar, S. G. (2006) Assembly of single bacteriorhodopsin trimers in bilayer nanodiscs. *Arch. Biochem. Biophys. 450*, 215−222.
(22) Bayburt, T. H., and Sligar, S. G. (2003) Self-assembly of single integral membrane proteins into soluble nanoscale phospholipid bilayers. *Protein Sci. 12*, 2476−2481.
(23) Whorton, M. R., Bokoch, M. P., Rasmussen, S. G., Huang, B., Zare, R. N., Kobilka, B., and Sunahara, R. K. (2007) A monomeric G protein-coupled receptor isolated in a high-density lipoprotein particle efficiently activates its G protein. *Proc. Natl. Acad. Sci. U.S.A. 104*, 7682−7687.
(24) Boldog, T., Grimme, S., Li, M., Sligar, S. G., and Hazelbauer, G. L. (2006) Nanodiscs separate chemoreceptor oligomeric states and reveal their signaling properties. *Proc. Natl. Acad. Sci. U.S.A. 103*, 11509−11514.
(25) Mi, L. Z., Grey, M. J., Nishida, N., Walz, T., Lu, C., and Springer, T. A. (2008) Functional and structural stability of the epidermal growth factor receptor in detergent micelles and phospholipid nanodiscs. *Biochemistry 47*, 10314−10323.
(26) Ye, F., Hu, G., Taylor, D., Ratnikov, B., Bobkov, A. A., McLean, M. A., Sligar, S. G., Taylor, K. A., and Ginsberg, M. H. (2010) Recreation of the terminal events in physiological integrin activation. *J. Cell Biol. 188*, 157−173.
(27) Perrault, C., Moog, S., Rubinstein, E., Santer, M., Baas, M. J., de la Salle, C., Ravanat, C., Dambach, J., Freund, M., Santoso, S., Cazenave, J. P., and Lanza, F. (2001) A novel monoclonal antibody against the extracellular domain of GPIbβ modulates vWF mediated platelet adhesion. *Thromb. Haemostasis 86*, 1238−1248.
(28) Auton, M., Cruz, M. A., and Moake, J. (2007) Conformational stability and domain unfolding of the von Willebrand factor A domains. *J. Mol. Biol. 366*, 986−1000.
(29) Fox, J. E. (1985) Linkage of a membrane skeleton to integral membrane glycoproteins in human platelets. Identification of one of the glycoproteins as glycoprotein Ib. *J. Clin. Invest. 76*, 1673−1683.
(30) Berndt, M. C., Gregory, C., Kabral, A., Zola, H., Fournier, D., and Castaldi, P. A. (1985) Purification and preliminary characterization of the glycoprotein Ib complex in the human platelet membrane. *Eur. J. Biochem. 151*, 637−649.
(31) Hess, D., Schaller, J., Rickli, E. E., and Clemetson, K. J. (1991) Identification of the disulphide bonds in human platelet glycocalicin. *Eur. J. Biochem. 199*, 389−393.
(32) Denisov, I. G., Baas, B. J., Grinkova, Y. V., and Sligar, S. G. (2007) Cooperativity in cytochrome P450 3A4: Linkages in substrate binding, spin state, uncoupling, and product formation. *J. Biol. Chem. 282*, 7066−7076.
(33) Fox, J. E., Aggerbeck, L. P., and Berndt, M. C. (1988) Structure of the glycoprotein Ib-IX complex from platelet membranes. *J. Biol. Chem. 263*, 4882−4890.
(34) Shen, Y., Romo, G. M., Dong, J. F., Schade, A., McIntire, L. V., Kenny, D., Whisstock, J. C., Berndt, M. C., Lopez, J. A., and Andrews, R. K. (2000) Requirement of leucine-rich repeats of glycoprotein (GP) Ibα for shear-dependent and static binding of von Willebrand factor to the platelet membrane GP Ib-IX-V complex. *Blood 95*, 903−910.
(35) Ward, C. M., Andrews, R. K., Smith, A. I., and Berndt, M. C. (1996) Mocarhagin, a novel cobra venom metalloproteinase, cleaves the platelet von Willebrand factor receptor glycoprotein Ibα. Identification of the sulfated tyrosine/anionic sequence Tyr-276-Glu-282 of glycoprotein Ibα as a binding site for von Willebrand factor and α-thrombin. *Biochemistry 35*, 4929−4938.
(36) Andrews, R. K., Booth, W. J., Gorman, J. J., Castaldi, P. A., and Berndt, M. C. (1989) Purification of botrocetin from *Bothrops jararaca* venom. Analysis of the botrocetin-mediated interaction between von Willebrand factor and the human platelet membrane glycoprotein Ib-IX complex. *Biochemistry 28*, 8317−8326.
(37) Hoylaerts, M. F., Nuyts, K., Peerlinck, K., Deckmyn, H., and Vermylen, J. (1995) Promotion of binding of von Willebrand factor to platelet glycoprotein Ib by dimers of ristocetin. *Biochem. J. 306*, 453−463.
(38) Meyer, S., Kresbach, G., Haring, P., Schumpp-Vonach, B., Clemetson, K. J., Hadvary, P., and Steiner, B. (1993) Expression and characterization of functionally active fragments of the platelet glycoprotein (GP) Ib-IX complex in mammalian cells. Incorporation of GP Ibα into the cell surface membrane. *J. Biol. Chem. 268*, 20555−20562.
(39) Mo, X., Luo, S.-Z., Munday, A. D., Sun, W., Berndt, M. C., Lopez, J. A., Dong, J.-f., and Li, R. (2008) The membrane-proximal intermolecular disulfide bonds in glycoprotein Ib influence receptor binding to von Willebrand factor. *J. Thromb. Haemostasis 6*, 1789−1795.
(40) Perrault, C., Mangin, P., Santer, M., Baas, M. J., Moog, S., Cranmer, S. L., Pikovski, I., Williamson, D., Jackson, S. P., Cazenave, J. P., and Lanza, F. (2003) Role of the intracellular domains of GPIb in controlling the adhesive properties of the platelet GPIb/V/IX complex. *Blood 101*, 3477−3484.
(41) Biaselle, C. J., and Millar, D. B. (1975) Studies on Triton X-100 detergent micelles. *Biophys. Chem. 3*, 355−361.
(42) Tsukamoto, H., Sinha, A., DeWitt, M., and Farrens, D. L. (2010) Monomeric rhodopsin is the minimal functional unit required for arrestin binding. *J. Mol. Biol. 399*, 501−511.
(43) Murata, M., Ware, J., and Ruggeri, Z. M. (1991) Site-directed mutagenesis of a soluble recombinant fragment of platelet glycoprotein Ibα demonstrating negatively charged residues involved in von Willebrand factor binding. *J. Biol. Chem. 266*, 15474−15480.
(44) Mo, X., Lu, N., Padilla, A., López, J. A., and Li, R. (2006) The transmembrane domain of glycoprotein Ibβ is critical to efficient expression of glycoprotein Ib-IX complex in the plasma membrane. *J. Biol. Chem. 281*, 23050−23059.
(45) Luo, S. Z., and Li, R. (2008) Specific heteromeric association of four transmembrane peptides derived from platelet glycoprotein Ib-IX complex. *J. Mol. Biol. 382*, 448−457.

(46) Calverley, D. C., Kavanagh, T. J., and Roth, G. J. (1998) Human signaling protein 14-3-3ζ interacts with platelet glycoprotein Ib subunits Ibα and Ibβ. *Blood 91*, 1295−1303.
(47) Mangin, P., David, T., Lavaud, V., Cranmer, S. L., Pikovski, I., Jackson, S. P., Berndt, M. C., Cazenave, J. P., Gachet, C., and Lanza, F. (2004) Identification of a novel 14-3-3ζ binding site within the cytoplasmic tail of platelet glycoprotein Ibα. *Blood 104*, 420−427.
(48) David, T., Ohlmann, P., Eckly, A., Moog, S., Cazenave, J. P., Gachet, C., and Lanza, F. (2006) Inhibition of adhesive and signaling functions of the platelet GPIb-V-IX complex by a cell penetrating GPIbα peptide. *J. Thromb. Haemostasis 4*, 2645−2655.